Carbohydrate Polymers 98 (2013) 922–930

Contents lists available at SciVerse ScienceDirect

Carbohydrate Polymers

journal homepage: www.elsevier.com/locate/carbpol

Purification, structure, lipid lowering and liver protecting effects of polysaccharide from *Lachnum* YM281

Tao Qiu, Xiaojing Ma, Ming Ye*, Ruyue Yuan, Yanna Wu

Microbial Resources and Application Laboratory, College of Biotechnology and Food Engineering, Hefei University of Technology, Hefei 230009, China

ARTICLE INFO

Article history:
Received 7 March 2013
Received in revised form 3 July 2013
Accepted 7 July 2013
Available online 12 July 2013

Keywords:
Lachnum YM281
Extracellular polysaccharide
Structure
Lipid lowering
Liver protecting

ABSTRACT

The extracellular polysaccharide (LEP) produced by *Lachnum* YM281 was obtained from the fermentation broth, and LEP-1b with molecular weight of 4.02×10^4 Da was separated and sequentially purified through DEAE-cellulose 52 column chromatography and Sepharose CL-6B column chromatography. GC–MS, IR and NMR (^{1}H, ^{13}C) spectroscopy analysis indicated that the repeat unit of LEP-1b was:

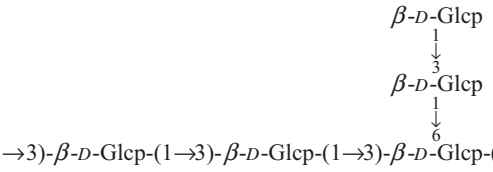

The effects of LEP-1b on the serum lipids, liver lipids levels and aminotransferase activities of model mice with hyperlipidemic fatty live were studied, and the results showed that LEP-1b had strong lipid lowering and liver protecting effects on mice with hyperlipidemic fatty live.

1. Introduction

Fungal polysaccharides, including glucan, mannan and heteropolysaccharide, etc., are known to present a broad range of biological activities, such as antioxidant, hypoglycemic, hypolipidemic, and liver protecting, etc., and have potential applications in the fields of heath products and drugs (He & Zhang, 2004; Li, Zhang, & Ma, 2010; Tseng, Yang, & Mau, 2008). In recent years, the chemical structures, chain conformations and biological activities relationships of fungal polysaccharides have drawn much attention. Suarez et al. (2006) reported that arabinogalactan with higher molecular weight exhibited immunostimulatory activity, while one with lower molecular weight did not. The bioactivities of fungal polysaccharides are also associated with the helical structures. It was reported that the immunoregulation and antitumor activities of some fungal polysaccharides, such as (1 → 3)-β-D-glucan form *Pleurotus florida*, *Ganoderma lucidum* or *Amanita muscaria*, are related to the triple helical conformation (Bao, Wang, Dong, Fang, & Li, 2002; Rout, Mondal, Chakraborty, & Islam, 2008).

One key factor causing atherosclerosis, fatty liver and cardiocerebrovascular disease is the hyperlipidemia, hence, consumption of polysaccharides with anti-hyperlipidemia activity could reduce the risk of associated diseases (Thongngam & McClements, 2005). High-fat food has a potential damage to liver, and when liver is damaged, a great amount of fat will accumulate in liver cells, resulting in fatty liver (Li et al., 2010; Wang, Cui, & Wei, 2010). Hence, in the prevention or treatment of fatty liver and liver injury, the main method is to lower the hepatic lipid and cholesterol levels.

Some *Lachnum* polysaccharides produced by saprophytic fungi of *Lachnum* sp. was reported to have antioxidant and hyperglycemic activities by our laboratory (Ye, Li, Yang, Zhu, & Lin, 2009; Ye et al., 2011). We have also reported the backbone chains of the extracellular polysaccharides of *Lachnum calyculiforme* and *Lachnum* YM261 are (1 → 3)-β-D-glucan, however, the structure of branch chains and conformation of the lachnum polysaccharides remains unclear. In the present study, specific structure of the *Lachnum* YM281 extracellular polysaccharide were characterized by GC–MS, IR and NMR spectroscopy analysis, and lipid lowering and liver protecting activities of LEP-1b were also demonstrated.

2. Materials and methods

2.1. Materials and reagents

Sepharose CL-6B and standard glucose were purchased form Sigma Chemical Co. (St. Louis, MO, USA). DEAE-cellulose 52 was purchased from Whatman Co. (Maidstone, Kent, UK). Standard

* Corresponding author at: College of Biotechnology and Food Engineering, Hefei University of Technology, Hefei 230009, China. Tel.: +86 0551 62919368; fax: +86 0551 62919368.
E-mail address: yeming123@sina.com (M. Ye).

0144-8617/$ – see front matter © 2013 Elsevier Ltd. All rights reserved.
http://dx.doi.org/10.1016/j.carbpol.2013.07.014

glucans with different molecular weight were obtained from Shodex Co. (Tokyo, Japan). TC, TG, LDL-C, HDL-C, ALT, AST, MDA and SOD kits were all purchased from Nanjing Jiancheng Bioengineering Institute (Nanjing, China). Female Kunming mice (initial weight at 20 ± 2 g) were purchased from Experimental Animal Center of Anhui Medical University, Hefei, China (Certificate number: Experimental Animal Standard No. 1 of Anhui Hospitals). The mice were kept at 23 ± 2 °C with a humidity of 55 ± 5% and a light-dark cycle of 14 h:10 h. The high fat diet consisting of 78.6% standard laboratory diet, 10% egg yolk, 10% pig fat, 1% cholesterol, 0.2% sodium cholate and 0.2% methylthiouracil was prepared by our laboratory (Li et al., 2010; Yu et al., 2003). Common-used lipid lowering drug of simvastatin was purchased form Merck & Co., Inc. (NJ, USA). Other chemicals and reagents were of analytical grade and purchased from Shanghai Zhenqi Chemical Reagent Co., Ltd. (Shanghai, China).

2.2. Microorganism and cultivation

The fruiting bodies of *Lachnum* YM281 were collected from Huangshan Mountain, Anhui, China. *Lachnum* YM281 was isolated by our laboratory and preserved in China Center for Type Culture Collection (CCTCC) with the collection number of M 2011196.

Fermentation medium contained glucose 3.0%, yeast extract 0.5%, KH_2PO_4 0.1%, $MgSO_4{\cdot}7H_2O$ 0.1% and vitamin B_1 0.005%. The activated strain was inoculated in a 250 mL Erlenmeyer flask containing 50 mL fermentation medium at 180 rpm, 25 °C for 4 days. Then the seed medium was transferred to a 5 L fermentor containing 3.5 L fermentation medium and cultivated for 10 days at 180 rpm, 25 °C.

2.3. Extraction and purification of LEP-1b

Three-fold volume of 95% ethanol was mixed with fermentation broth after its suction filtration and concentration. Then the solution was precipitated at 4 °C for 12 h before centrifuged for 10 min at 4000 rpm. After supernatant was removed, sediment was dissolved with distilled water. Crude extracellular polysaccharides were obtained after freeze-drying. Before purification, the crude extracellular polysaccharides of *Lachnum* YM281 was decolored and deproteinized by our previous method (Ye et al., 2011).

DEAE-cellulose 52 column chromatography and Sepharose CL-6B column chromatography was applied to fractionate the polysaccharides in order. Firstly, crude polysaccharides (100 mg) was re-dissolved in 5 mL distilled water and applied to a DEAE-cellulose 52 column (1.6 cm × 60 cm) equilibrated with distilled water. Then, the polysaccharide was fractionated and eluted with different concentrations of stepwise NaCl solutions (0, 0.1, 0.5 M) at a flow rate of 0.5 mL/min. The main fraction (20 mg) was obtained and then further fractionated by Sepharose CL-6B column (1.6 cm × 60 cm) chromatography with 0.9% NaCl solution at a flow rate of 0.55 mL/min. The samples were partly collected using an automated step-by-step fraction collector and detected tube by tube by the phenol–sulfuric acid method using glucose as the standard, and the elution curves were plotted. As results, three fractions of polysaccharides (LEP-1, LEP-2 and LEP-3) were obtained. LEP-1 was concentrated, dialyzed and further purified through a column of Sepharose CL-6B to isolate LEP-1a and LEP-1b. The resulted LEP-1b was the main component of the crude polysaccharide of *Lachnum* YM281 and was then concentrated, dialyzed and lyophilized for further study.

2.4. Determination of homogeneity, molecular weight and monosaccharide component of LEP-1b

The homogeneity and molecular weight of LEP-1b were determined by high performance liquid gel permeation chromatography (HPGPC) according to the methods reported by Ye et al. (2011). Glucans with different molecular weight were used as standards for molecular weight measurement. The molecular mass was calculated according to the calibration curve of standard dextrans. The monosaccharide component of LEP-1b was obtained by acetylation reaction followed by GC–MS analysis.

2.5. Structure elucidation of LEP-1b

2.5.1. Periodate oxidation and Smith degradation

LEP-1b (25 mg) was dissolved in 25 mL of 15 mM $NaIO_4$ solution and the mixture was kept in the dark at 4 °C. Subsequently, 500 μL of reactive mixture were taken out every 6 h, diluted 200 times with distilled water, and read in a spectrophotometer at 223 nm until the absorbance to a constant value. Ethylene glycol (1 mL) was added to terminate the reaction. The periodic acid consumption was calculated based on the standard curve of $NaIO_4$. Reaction mixture of 2 mL was titrated with 0.001 M NaOH solution to determine the production of formic acid.

After periodic acid oxidation, the reaction mixture was added with ethylene glycol (1 mL), dialyzed against distilled water for 48 h, reduced by 80 mg of $NaBH_4$ addition in the dark for 24 h. Then, the reaction mixture was neutralized with 0.1 M acetic acid and dialyzed against distilled water again. The dialyzed product was dried, hydrolyzed, acetylated and analyzed by GC–MS analysis according to our previous method (Ye et al., 2011). GC–MS conditions: silica capillary column: HP-5 (30 m × 0.25 mm × 0.25 μm); temperature program: initially at 50–250 °C at a rate of 10 °C/min and then held for 20 min; inlet temperature: 260 °C; ion source: EI, 70 eV; molecular weight: 35–650 amu s^{-1}; helium flow speed: 1 mL/min.

2.5.2. Methylation analysis

The method descried by Needs and Selvendran (1993) with minor modification was used for methylation reaction. Briefly, amounts of 28.5 mg LEP-1b was dissolved in 0.15 mL water, and then mixed with 4.5 mL of DMSO and 1 g of 3 A molecular sieve. After blending and sealing, the container with the above mixture was placed in a desiccator for 24 h to remove water. Then the mixture was filtered into the reaction flask in dry environment. The reaction solution was added with 75 mg of NaOH powder, aerated with N_2, and treated with ultrasound for 30 min at room temperature. After that, the reaction solution was added with 0.75 mL of CH_3I, aerated with N_2, and treated with ultrasound for 2 h at room temperature. N_2 was aerated to remove the remained CH_3I. Completely methylated polysaccharide was obtained by repeating above procedure for three times. Water (2 mL) was added to terminate the reaction. The reaction solution was neutralized with 1 M acetic acid, dialyzed 48 h against distilled water, and dried. IR spectroscopy was applied to check whether the polysaccharide was completely methylated (without absorption peak at 3400 cm^{-1}). The methylated polysaccharide was hydrolyzed, derived and analyzed by GC–MS followed the method described in Section 2.5.1.

2.5.3. Partial acid hydrolysis

Partial acid hydrolysis of LEP-1b was proceeded according to the method by Tong et al. (2009) with minor modification. LEP-1b (80 mg) was hydrolyzed with 8 mL of 0.05 M trifluoroacetic acid (TFA) for 16 h at 95 °C, and dialyzed for 48 h against distilled water after TFA was removed. The products in and outside the dialysis sack were collected respectively. Followed by concentrated and dried, the products were fractionated by Sephadex G-100 column (1.6 cm × 60 cm) chromatography eluted with distilled water at a flow rate of 0.2 mL/min (Ye et al., 2011). Finally, the obtained components were completely methylated, hydrolyzed, acetylated, and

analyzed by GC–MS using the same method described in Section 2.5.1.

2.5.4. UV, IR and NMR analysis

The purified LEP-1b was applied to ultraviolet (UV) spectrum, infrared spectrum (IR) and nuclear magnetic resonance (NMR) analysis. UV spectrum was recorded by scanning the LEP-1b solution (5 mg/mL) in a Shimadzu MPS-2000 spectrophotometer (Shimadzu, Japan) with wavelength of 190–400 nm. To detect functional groups of LEP-1b, IR spectrum were obtained with Nexus-6700 Fourier-transform infrared spectrometer (Thermo Nicolet, USA). LEP-1b was ground, mixed with KBr powder (1/100), pressed into pellets and detected in the frequency range of 4000–400 cm^{-1}. Bruker AV-500 spectrometer (Bruker, Germany) was used for ^{1}H NMR and ^{13}C NMR analysis with the frequency of 500.13 MHz for ^{1}H NMR and 125.76 MHz for ^{13}C NMR, the temperature of 300 K and the delay time of 2 s. Chemical shifts were given in ppm.

2.5.5. Congo red reaction

Conformation structure of LEP-1b was analyzed by Congo red reaction according to the method described by He, Shao, Men, and Sun (2010) with minor modification. The mixture solutions of the LEP-1b (0.5 mg/mL) in 0–0.5 M NaOH (increasing stepwise by 0.05 M increments) containing 91 μM of Congo red were prepared and analyzed with a UV-VIS spectrophotometer (HP, USA) in the range of 400–700 nm, and the maximum absorption wavelengths were recorded as a function of NaOH concentration. Congo red in NaOH served as the negative control.

2.6. Lipid lowering and liver protecting effects of LEP-1b

2.6.1. Animal and treatments

Ninety female Kunming mice weighting 20 ± 2 g were used in the animal experiments. After a week of adaptive feed, the mice were randomly divided into 6 groups with 15 animals in each group: high-dose LEP-1b group (200 mg/kg), medium-dose LEP-1b group (100 mg/kg), low-dose LEP-1b group (50 mg/kg), normal control group, model control group, and positive control group (7 mg/kg simvastatin).

To establish model mice with hyperlipidemic fatty liver, normal control group was given standard laboratory diet and the other 5 groups were fed with high fat diet for 2 weeks. After diet inducing, 4 mice from the control group and each model group were selected randomly, respectively. Blood samples were collected by removing the eye balls, and centrifuged at 4000r/min for 10 min at 4 °C. The serum was obtained and preserved at −20 °C. Livers were quickly excised, weighed and preserved at −80 °C until analysis. Then, total cholesterol (TC), triglyceride (TG), low-density lipoprotein cholesterol (LDL-C) and high-density lipoprotein cholesterol (HDL-C) in serum and liver of the selected mice were determined respectively. The results showed that, when compared with control group, the serum and liver TC, TG, LDL-C and fat contents were increased significantly after 2 weeks of high fat feeding ($p < 0.01$). The liver was soft and exhibited color of gray-yellow or pale. The liver cut surface was greasy, showing obvious fatty liver symptoms. The above results indicated that model mice with hyperlipidemic fatty liver had been successfully established (Ding, Gao, Chao, & Xia, 2010).

From the 3rd week, mice of the three LEP-1b groups were given with LEP-1b at the doses of 50,100 and 200 mg/kg respectively by gavage. Mice of the normal control group and model control group were given normal saline of the same volume, once a day for 4 weeks consecutively. For mice of positive control group, 7 mg/kg of simvastatin was given by gavage. During the administration period, normal control group was fed with standard laboratory diet and the other 5 groups were fed with high fat diet. Food intakes were measured every day, body weights were weighed every week, and excrements were collected during the last 3 days of experiment.

Mice of each groups were kept fasting for 12 h before the last gavage. Blood were collected one hour after the last gavage by enucleating eye balls, and serum was prepared by centrifugation at 4000 rpm for 10 min and preserved at −20 °C until analysis. Livers were quickly excised, weighed and preserved at −80 °C until analysis. The liver index (g/100 g bw) was calculated as liver weight (g)/body weight (100 g).

2.6.2. Measurement of lipids in serum and liver

The TC, TG, HDL-C and LDL-C levels in serum were determined using relevant diagnostic kits, and atherogenic index (AI) was calculated as (TC − HDL-C)/HDL-C (Queiroz-Monici, Costa, Silva, Reis, & Oliveira, 2005).

The lipid in the liver tissue was extracted according to a previously reported method with minor modifications (Ding et al., 2010). The contents of liver TC and TG were determined with kits. After vacuum freeze-drying, the liver tissue was ground for the determination of liver fat content with Soxhlet extraction.

2.6.3. Determination of ALT, AST and SOD activities and MDA content

The serum alanine aminotransferase (ALT), aspartate aminotransferase (AST), liver superoxide dismutase (SOD) activities and liver methane dicarboxylic aldehyde (MDA) content were determined using commercial kits followed the kits instructions.

2.6.4. Measurement of TBA, TC and fat excretions in excrement

The excrement of mice was weighed after freeze-drying. Then total bile acid (TBA) content in excrement was determined by the method of Wilson, Nicolosi, Rogers, Sacchiero, and Goldberg (1998). Method raised by Kritchevsky and Tepper (2005) was used to extract and determine the fat content in excrement. The TC content of excrement was determined using kit. TBA (TC or fat) excretion (mg/mouse/3 days) = excrement mass × TBA (TC or fat) content.

2.6.5. Morphological observation of liver tissue

Fresh liver tissue masses (about 2 cm × 2 cm × 0.2–0.3 cm) were embedded in optimal cutting temperature (OCT) tissue freezing medium and then sliced with freezing microtome with the thickness of 8 μm. The sections were fixed in 10% formalin solution for 1 min for conventional HE staining, and then observed with an optical microscope, and photos were taken.

2.6.6. Statistical analysis

All data were expressed by mean ± SD after statistical analysis. Software of SPSS13.0 was used for t-test of differences between groups. Differences were considered statistically significant when $p < 0.05$ and extremely statistically significant when $p < 0.01$.

3. Result and discussion

3.1. Isolation, purification and molecular weight of LEP-1b

Crude LEP was prepared from the fermentation broth of *Lachnum* YM281 by concentration, alcohol precipitation, deproteinization, decoloration and dialysis. The production of LEP reached 6.38 g/L in the fermentation medium. Then, the crude LEP was firstly fractionated through an anion-exchange chromatography of Cellulose DEAE-52 to obtain three independent elution fractions of LEP-1, LEP-2 and LEP-3 (Fig. 1A). The neutral polysaccharide (LEP-1), the main fraction of the crude LEP, was eluted by distilled water. The fraction of LEP-1 was collected, concentrated and fractionated by Sepharose CL-6B column chromatography. As

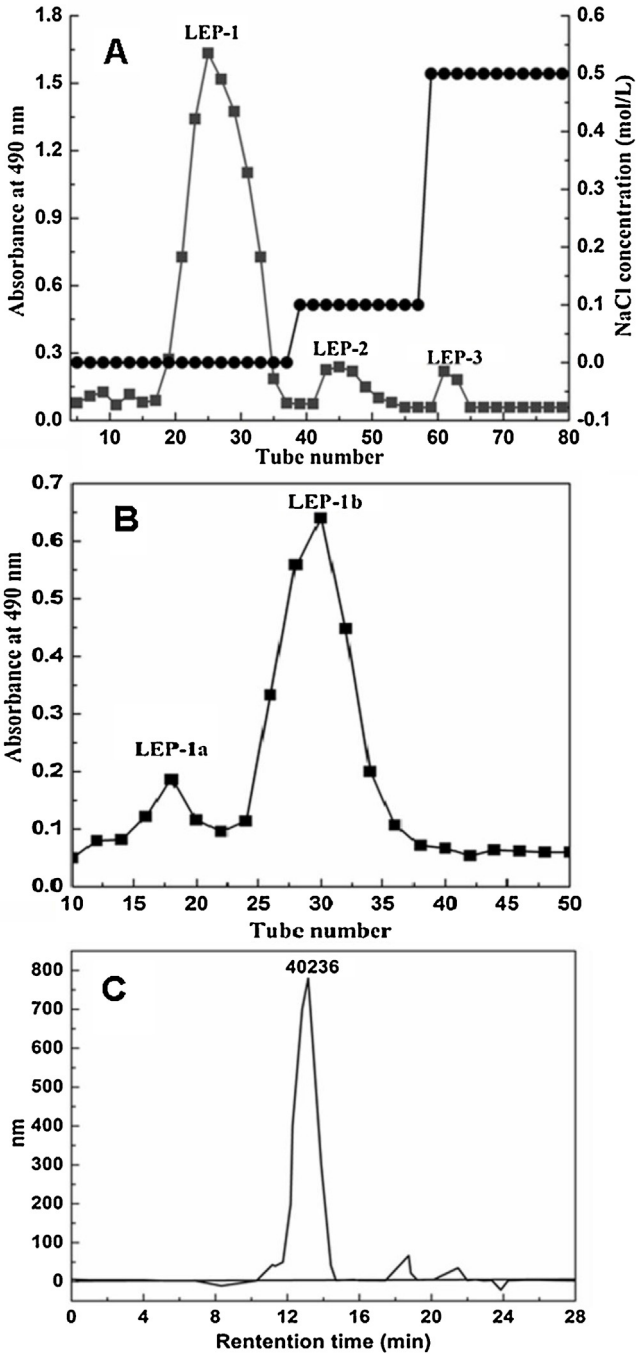

Fig. 1. Chromatography of LEP on Cellulose DEAE-52 Column (A), LEP-1 on Sepharose CL-6B column (B) and high performance liquid gel permeation chromatogram of LEP-1b (C).

a result, two fractions of LEP-1a and LEP-1b were obtained, respectively (Fig. 1B). Main fraction of LEP-1b was collected, dialyzed and dried. Single symmetrical elution peak of LEP-1b by HPGPC showed that LEP-1b was a homogeneous component and no other polysaccharide was present. According to the calibration curve of the elution times of standards, the molecular weight of LEP-1b was estimated to be 4.02×10^4 Da (Fig. 1C).

3.2. Structure elucidation of LEP-1b

After hydrolysis of LEP-1b with TFA and acetylation, the monosaccharide composition of the LEP-1b was analyzed by GC–MS. Sole peak at the retention time of 19.296 min was observed on its total ion chromatogram (TIC) and its mass spectral data was consistent with that of acetyl derivative of glucose. The presence of single sugar moiety suggested that the LEP-1b was a glucan only composed of glucose.

The results of periodate oxidation showed that LEP-1b consumed 0.29 mol of periodate and produced 0.14 mol of formic acid per mole of glucosyl residues with a molar ratio of 2.07:1. This suggested the existence of 1→ or 1 → 6 glycosidic linkages and inexistence of 1 → 2, 1 → 4, 1,2 → 6, 1,4 → 6 glycosidic linkages, which could consume periodate but produce no formic acid (He et al., 2010). No erythritol was observed, and a large amount of glucose and certain amount of glycerol were detected from GC–MS data of derivatives from LEP-1b after periodate oxidation and Smith degradation. Glucose was the main product in the Smith degradation of LEP-1b, which indicated that a great amount of glycosidic linkages, such as 1 → 3, 1, 3 → 6, 1, 2 → 3 and 1, 2 → 4 existed in LEP-1b were not oxidated in periodate oxidation. Formation of glycerol also revealed that 1→ or 1 → 6 glycosidic linkages were existed in LEP-1b (Wang, Yin, Lv, Gao, & Wang, 2010).

The methylated product of LEP-1b was hydrolyzed, acetylated and analyzed by GC–MS. As shown in Table 1, 2,3,4,6-Me_4-Glc, 2,4,6-Me_3-Glc and 2, 4-Me_2-Glc were detected with molecular ratio of 1.07:5.15:1.00 and retention time of 17.023 min, 18.665 min and 19.493 min, respectively. The high proportion of 2,4,6-Me_3-Glc implied that the backbone chain of LEP-1b was composed of 1,3-linked Glc. The presence of 2,4-Me_2-Glc revealed the existence of 1,3,6-linked Glc, indicating that there was a branch chain in LEP-1b, and the branched chain was linked at C_6 of the backbone chain of the glucan. 2,3,4,6-Me_4-Glc indicated the existence of the non-reducing terminal glucose residues (Dong, Jia, & Fang, 2006).

The partial acid hydrolysis products of LEP-1b were dialyzed and the products in and outside the dialysis sack were concentrated and dried, respectively. Both of components in the dialysis sack (backbone chain, named as LEP-1b-1) and outside the dialysis sack (branch chain, named as LEP-1b-2) were detected to be homogeneous component by Sephadex G-100 column chromatography. LEP-1b-1 and LEP-1b-2 were analyzed with the method of methylation analysis. The results listed in Table 1 showed that LEP-1b-1 was composed of 1,3-linked Glc and 1,3,6-linked Glc with a molecular ratio of 1:3.96, and LEP-1b-2 was composed of 1,3-linked Glc and terminal Glc with a molecular ratio of 1:1.08. Combining the results of methylation analysis, LEP-1b was speculated to consist of glucose residues linked by 1 → 3 glycosidic linkage, and each repeat unit was constituted by seven glucose residues. That is, in each repeat unit of LEP-1b, there were one backbone chain (five glucose residues linked by 1 → 3 linkage) and one branch chain (two glucose residues linked by 1 → 3 linkage), and the branch chain was linked at C_6 of the backbone chain by 1 → 6 linkage.

No absorption peak was observed between 260 and 280 nm in the UV spectrogram of LEP-1b. This suggested that there was no protein or nucleic acid in the purified LEP-1b (Sun & Liu, 2009). The FT-IR spectrogram of LEP-1b was shown in Fig. 2, the absorption peak at 3394.10 cm^{-1} represented the O—H stretching vibration. The peak at 2937.06 cm^{-1} was induced by C—H stretching vibration. The intense absorption band at 1654 cm^{-1} corresponds to the bending mode of the absorbed water in LEP-1b (Shi, Xiao, Deng, Xu, & Sun, 2011). The band at 1421 cm^{-1} was attributed to bending vibration of C—H or O—H (Cao, Yuan, Sun, & Sun, 2011). And the absorption peaks between 1250 and 950 cm^{-1} indicated that the sugar rings were pyranose rings (Sun, Liu, Yang, & Kennedy, 2010; Zou, Zhang, Yao, Niu, & Gao, 2010).

^{1}H NMR spectrum of LEP-1b was shown in Fig. 3. The signal peaks between 3.57 ppm and 4.14 ppm suggested the existence of sugar rings. The chemical shift of H_1 proton (less than 4.95 ppm) indicated that sugar rings of LEP-1b were pyranose rings and

Table 1
GC–MS data for methylation analysis of LEP-1b, LEP-1b-1 and LEP-1b-2.

Group	Methylated sugar	MS data of main fragments, *m*/*z*	Linkage type	Molar ratio
LEP-1b	2,3,4,6-Me_4-Glc	43, 45, 71, 87, 101, 117, 129, 145, 161, 205	Terminal Glc	1.07
	2,4,6-Me_3-Glc	43, 45, 87, 101, 117, 129, 139, 161	1,3-Linked Glc	5.15
	2,4-Me_2-Glc	43, 71, 87, 101, 117, 129, 139, 161, 189	1,3,6-Linked Glc	1.00
LEP-1b-1	2,4-Me_2-Glc	43, 71, 87, 101, 117, 129, 139, 161, 189	1,3,6-Linked Glc	1.00
	2,4,6-Me_3-Glc	43, 45, 87, 101, 117, 129, 139, 161	1,3-Linked Glc	3.96
LEP-1b-2	2,4,6-Me_3-Glc	43, 45, 87, 101, 117, 129, 139, 161	1,3-Linked Glc	1.00
	2,3,4,6-Me_4-Glc	43, 45, 71, 87, 101, 117, 129, 145, 161, 205	Terminal Glc	1.08

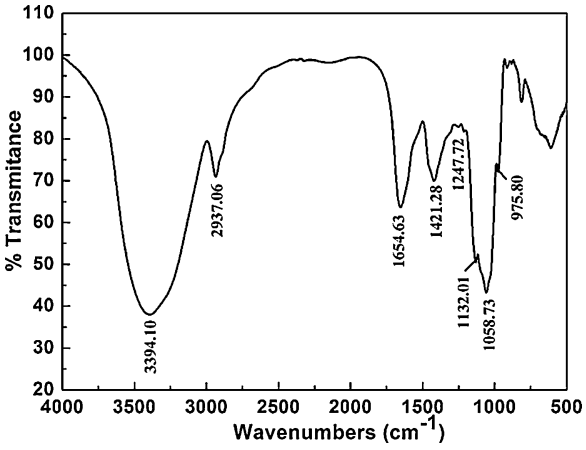

Fig. 2. The IR spectra of LEP-1b.

saccharide residues were linked by β-glycosidic linkage (Li, Fan, & Ding, 2011). ^{13}C NMR spectrum (Fig. 4) showed that the anomeric carbon signal of δ102.82 was generated by C_1 of →3)-β-*D*-Glcp-(1→ and indicated the sugar rings conformation was Pyran type (Wang, Cui, et al., 2010; Wang, Yin, Lv, Gao, & Wang, 2010). The chemical shifts of C_2, C_3, C_4, C_5 and C_6 were δ71.07, δ78.65, δ67.21, δ73.15 and δ63.68, respectively. The chemical shift of C_3, higher than 78 ppm, indicated that C_3 of glucose residues in LEP-1b were substituted C_3. The chemical shift of C_3 and C_6 at δ78.65 and δ63.68 suggested the existence of β-glucopyranose residues. In addition, the δ67.21 signal revealed the existence of →6)-β-*D*-Glcp-(1→, and the strong signal peak at δ63.68 implied that C_6 of most glucose residues in LEP-1b were un-substituted C_6 (He et al., 2010). These results of NMR spectra were consistent with that of IR analysis.

All the above results deduced that the backbone chain of LEP-1b was consisted of β-1,3-D-Pyran glucose residues, every five glucose residues constituted a repeat unit, and each repeat unit contained a branch chain (two *D*-Pyran glucose residues linked by β-1,3-linkage), which was linked at C_6 of the backbone chain by β-1,6-linkage. The proposed structure of repeat unit of LEP-1b was shown in Fig. 5. The glycosidic linkages of LEP-1b are almost the same as some active β-D-glucan linkages reported previously, whereas the branch chains and repeat units are different.

3.3. Conformational characterization of LEP-1b

It has been reported that (1 → 3)-β-D-glucans with a helical conformation can form complexes with Congo red in dilute alkaline solution as indicated by a shift in the maximum absorption wavelength (λ_{max}) of Congo red (Dong et al., 2006). A strong alkaline environment can destroy ordered helical structure into a disordered structure by breaking the intra- and inter-molecular hydrogen bonds. The greater the effect in the λ_{max} shift, the higher the helical structure content is (Rout et al., 2008). In this way, a shift in the maximum visible absorption of Congo red induced by the presence of a polysaccharide was used for conformational studies. As shown in Fig. 6, the λ_{max} of the mixture of Congo red and LEP-1b presented a shift of 15 nm (from 496 nm to 511 nm) in 0.1 M NaOH solution and the λ_{max} decreased with the increase of NaOH concentration. The curve was flattened at 503 nm and remained the same when the NaOH concentration was higher than 0.35 M. This result suggested that the LEP-1b had triple helix conformation and the ordered triple helix structure lost at concentrations of 0.35 M NaOH and higher.

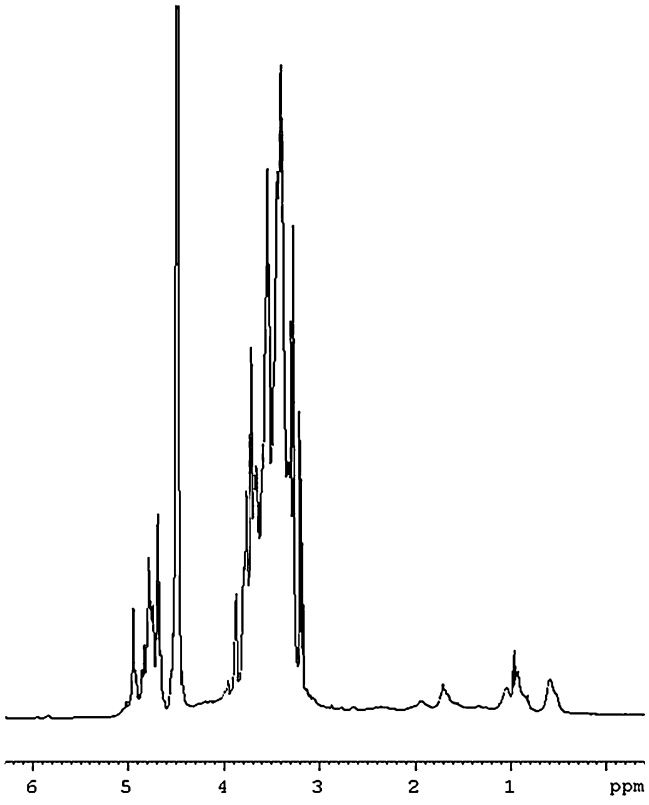

Fig. 3. The ^{1}H NMR spectra of polysaccharide LEP-1b at 27 °C.

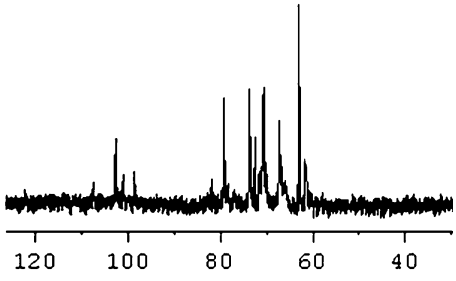

Fig. 4. The ^{13}C NMR spectra of polysaccharide LEP-1b at 27 °C.

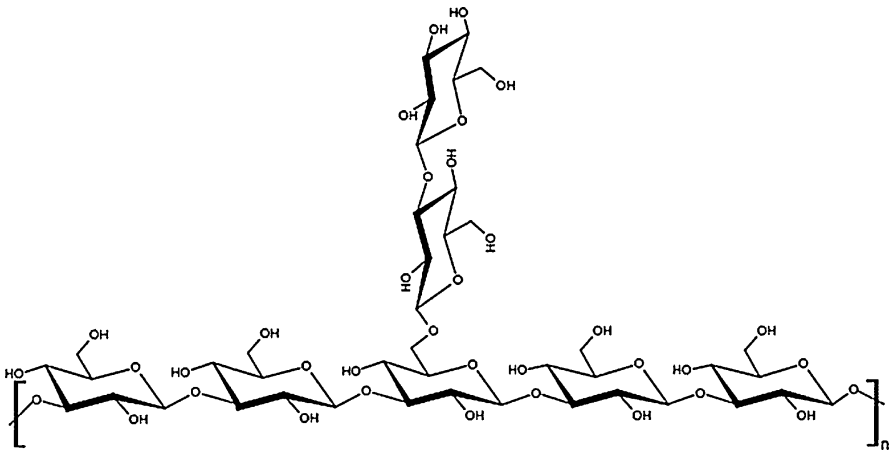

Fig. 5. The proposed structure of LEP-1b.

3.4. Lipid lowering and liver protecting effects determination of LEP-1b

3.4.1. Food intake and growth of mice

Compared with the normal control, mice in the model control showed a significant increase in the body weight gain and feeding efficiency ($p < 0.05$, $p < 0.01$, Table 2). Four weeks after being given administrations, the body weight gain and feeding efficiency of mice in the high-dose LEP-1b group, medium-dose LEP-1b group and positive control group were significantly lower than those in the model control group ($p < 0.01$ or $p < 0.05$), and there was no significant difference in the body weight gain and feeding efficiency between the high-dose LEP-1b mice and the normal control mice.

3.4.2. Lipid content in serum, liver and excrement

Blood–lipid reduction, hepatic lipid reduction and repair of damaged liver tissues play important roles in the prevention, alleviation and cure of hyperlipidemia, atherosclerosis and fatty liver, and are of great significance in reduction of the cardio-cerebrovascular disease incidence. Hence, to develop natural, low-toxic and high-efficient lipid-reducing and liver-protecting medicines is the international research focus at present. The TC, TG, LDL-C and HDL-C contents in serum are important indicators for analysis of lipid metabolism. TC and LDL-C contents being too high or HDL-C content being too low are the major symptoms of hyperlipidemia, and the abnormality of serum lipid also is the major risk factor of atherosclerosis (Li et al., 2010).

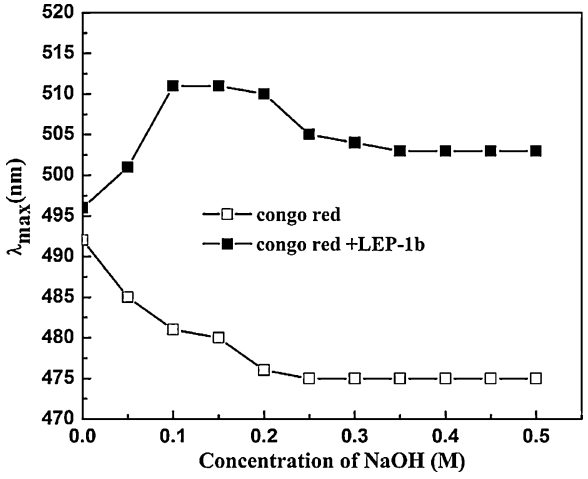

Fig. 6. Changes in the absorption maximum of the Congo red-LEP-1b complex at various concentrations of sodium hydroxide solution.

As shown in Table 3, the TC, TG and LDL-C contents in serum and AI of the model control mice were all significantly higher than those of the normal control mice ($p < 0.01$). There was only a slight decrease of HDL-C in mice fed the high fat diet, but this was insignificant when compared with that in mice fed the normal diet ($p > 0.05$). This phenomenon was in agreement with studies of Hu et al. (2010) and the possible reason was still unclear. After 4 weeks of lavage administration, the high-dose as well as medium-dose LEP-1b and the positive control drug of simvastatin all significantly lowered the TC, TG and LDL-C contents in serum and AI of the model mice, and significantly increased the serum HDL-C content ($p < 0.01$ or $p < 0.05$), exhibiting a dose–effect relationship. Compared with the model control mice, the TC, TG and LDL-C contents and AI of the high-dose LEP-1b mice declined by 58.39%, 19.65%, 76.22% and 78.51%, respectively, and the HDL-C content increased by 19.53%, whereas there was no significant difference in AI between the high-dose LEP-1b mice and the normal control mice. These results indicated that LEP-1b exhibited excellent blood–lipid level and atherogenic index lowering effects on model mice with hyperlipidemic fatty liver.

TC, TG and fat contents in liver are important indicators for analyzing of fatty liver. Cholesterol in the body is converted to bile acid mainly via liver and then excreted with feces. Bile acids, which were secreted into the intestine, are conducive to emulsification and absorption of lipids. Therefore, bile acid, cholesterol and fat contents in excrement are also important indicators for lipid metabolism situation analysis (Hu et al., 2010).

In this study, the TC, TG and fat contents in liver of the model control mice were significantly higher than those of the normal control mice (Table 3). After 4 weeks of lavage administration, the TC, TG and fat contents in liver of the high-dose as well as medium-dose LEP-1b mice and the positive control mice were all significantly lower than those of the model control mice ($p < 0.01$). The TC, TG and fat contents in liver of the high-dose LEP-1b mice decreased by 44.12%, 33.40% and 57.53% compared to the model control mice. And there was no significant difference in the liver TC, TG and fat contents among the high-dose, medium dose and low-dose LEP-1b groups and the normal control group. Additionally, the TBA, TC and fat excretions of the model control mice were all significantly higher than those of the normal control mice (Table 3). Four weeks after being given with administration, the TBA, TC and fat excretion of the high-dose LEP-1b mice and the positive control mice were both significantly higher than those of the model control mice ($p < 0.01$ or $p < 0.05$). The TBA and TC excretions of the high-dose

Table 2
Food intake and growth of mice in various groups.

Groups	Normal control	Model control	Positive control	LEP-1b (200 mg/kg)	LEP-1b (100 g/kg)	LEP-1b (50 mg/kg)
Initial body wt (g/m)	20.53 ± 1.04	20.20 ± 1.13	20.33 ± 1.09	20.36 ± 1.20	20.17 ± 1.33	20.49 ± 1.30
Final body wt (g/m)	30.95 ± 0.82	33.53 ± 1.02**	30.22 ± 1.67***	29.66 ± 0.58***,****	30.35 ± 2.34***	32.53 ± 0.71*
Weight gain (g/m/d)	0.25 ± 0.03	0.32 ± 0.03*	0.24 ± 0.06***	0.23 ± 0.03****	0.24 ± 0.04***	0.26 ± 0.05
Food intake (g/m/d)	3.32 ± 0.31	2.94 ± 0.28	3.10 ± 0.37	3.05 ± 0.32	2.94 ± 0.29	3.06 ± 0.40
Feeding efficiency (%)	7.50 ± 0.60	9.86 ± 0.78**	7.81 ± 1.20***	7.38 ± 0.74****	8.22 ± 0.98***	8.38 ± 1.11

Notes: Results are mean ± SD, $n \geq 10$. m, mouse.
* $p < 0.05$ vs. normal control group.
** $p < 0.01$ vs. normal control group.
*** $p < 0.05$ vs. model control group.
**** $p < 0.01$ vs. model control group.

LEP-1b group were 14.91% and 26.91% lower than those of the positive control group, respectively. However, the fat excretion of the high-dose LEP-1b group was 0.75% higher than that of the positive control group. There was no significant difference in the TBA, TC and fat excretion between the low-dose LEP-1b mice and the model control mice.

These results described above indicated that LEP-1b can effectively reduce the hepatic lipid level and enhance the excrement-lipid excretions of the model mice with hyperlipidemic fatty liver. The reason may be that LEP-1b has the activity of inhibiting the synthesis of HMG-CoA reductase from cholesterol, thus reducing the endogenous synthesis of cholesterol. Another reason may be that LEP-1b has the capacity of inhibiting the enterohepatic cycle of bile acids and enhancing the metabolism and decomposition of cholesterols through the way of up-regulating the expressions of ileum FXR and hepatic CYP7A1 genes and down-regulating the expressions of I-BABP and hepatic FXR. The third reason may be that the transcriptional up-regulation of PPARα, PPARγ, Lpl and Lpic leads to the decrease of the fat synthesis rate and the increase of the fat hydrolysis rate, thus accelerating the metabolism and decomposition of triglyceride (García-Mediavilla, Villares, Culebras, Bayón, & González-Gallego, 2003; Makishima et al., 1999; Takahashi et al., 2002). However, the specific mechanism of lipid lowering and liver protecting of LEP-1b need further investigation.

3.4.3. *Liver protecting activity of LEP-1b*

High fat food intake for a long time will cause triglyceride and cholesterol to synthesize faster than its transporting rate and accumulate in the liver cells, resulting in fatty liver. Fatty liver formation is related to the oxidative stress and lipid peroxidation in liver. Lipid peroxidation in liver interferes with liver lipid metabolism, causing lipid deposition, which again increases lipid peroxidation, damaging the liver cells, and thus leading to the significant increase of the serum ALT and AST activities and the liver MDA content and the significant reduction of the liver SOD activity (Luo et al., 2009; Percario et al., 2008).

In this study, it was found that the ALT and AST activities in serum of the model control mice were both significantly higher than those of the normal control mice (Table 3). After 4 weeks of lavage administration, the ALT and AST activities in mice serum of the LEP-1b groups and the positive control group were significantly lower than those of the model control group ($p < 0.01$), showing a good dose–effect relationship. The ALT and AST activities in mice serum of the high-dose LEP-1b group were 50.36% and 52.22% lower than those of the positive control group, respectively, and without significantly difference from those of the normal control group. Compared with the normal control group, the liver SOD activity of the model control mice had a significant decline, and the liver MDA content and liver index both showed a significant rise (Table 3). After 4 weeks of lavage administration, compared with the model

Table 3
Effect of LEP-1b in different doses on the serum, liver lipid, TBA, TC and fat excretions in excrement and repair effect of LEP-1b on the damaged liver of the model mice.

Index		Normal control	Model control	Positive control	LEP-1b (200 mg/kg)	LEP-1b (100 mg/kg)	LEP-1b (50 mg/kg)
Serum lipids (mmol/l)	TC	2.61 ± 0.24	7.45 ± 0.68**	2.91 ± 0.11****	3.10 ± 0.16*,****	3.77 ± 0.34**,****	6.62 ± 0.57**
	TG	0.99 ± 0.08	1.73 ± 0.14**	1.24 ± 0.13*,****	1.39 ± 0.13**,***	1.45 ± 0.10**,***	1.54 ± 0.17**
	HDL-C	1.32 ± 0.07	1.28 ± 0.12	1.61 ± 0.06**,****	1.53 ± 0.09*,***	1.50 ± 0.06**,***	1.41 ± 0.09
	LDL-C	0.84 ± 0.21	5.93 ± 0.66**	0.93 ± 0.15****	1.41 ± 0.05**,****	2.61 ± 0.26**,****	5.09 ± 0.58**
	AI	0.98 ± 0.14	4.84 ± 0.42**	0.81 ± 0.04****	1.04 ± 0.23****	1.51 ± 0.17**,****	3.71 ± 0.58**,***
Liver lipids (μmol/g, μmol/g, %)	TC	9.50 ± 0.46	40.19 ± 4.11**	13.27 ± 1.16**,****	22.46 ± 1.38**,****	29.03 ± 2.47**,****	33.85 ± 2.38**,***
	TG	4.88 ± 0.12	15.72 ± 1.00**	8.79 ± 0.60**,****	10.47 ± 0.59**,****	11.47 ± 0.84**,****	14.47 ± 0.76**
	Fat	9.95 ± 0.32	26.61 ± 0.76**	10.54 ± 1.05****	11.30 ± 0.86*,****	15.88 ± 0.65**,****	18.19 ± 0.67**,****
Excrement (mg/mouse/3 days)	TBA	33.67 ± 1.48	38.23 ± 1.81**	79.34 ± 4.18**,****	67.51 ± 3.90**,****	71.27 ± 4.63**,****	39.87 ± 1.96**
	TC	1.04 ± 0.12	9.33 ± 0.91**	29.73 ± 2.4**,****	21.73 ± 1.87**,****	17.37 ± 1.70**,****	10.36 ± 1.53**
	Fat	114.96 ± 11.72	279.22 ± 21.86**	331.58 ± 24.61**,***	334.08 ± 20.65**,***	295.24 ± 33.48**	277.75 ± 20.83**
Serum (U/L)	ALT	45.35 ± 1.85	123.64 ± 6.15**	93.33 ± 6.03**,****	46.33 ± 3.83****	49.08 ± 5.34****	63.08 ± 6.01*,****
	AST	40.69 ± 1.10	130.75 ± 8.32**	87.03 ± 3.82**,****	41.58 ± 2.36****	43.58 ± 1.83*,****	59.75 ± 4.15**,****
Liver (U/mg pro, nmol/mg pro, g/100 g bw)	SOD	233.29 ± 10.27	115.88 ± 6.17**	171.93 ± 9.22**,****	248.14 ± 4.91*,****	210.08 ± 11.99*,****	175.41 ± 9.19*,****
	MDA	1.17 ± 0.08	2.10 ± 0.09**	1.56 ± 0.09**,****	1.21 ± 0.08****	1.62 ± 0.07**,****	1.87 ± 0.10**,***
	Liver index	4.83 ± 0.20	6.88 ± 0.15**	4.72 ± 0.14****	4.88 ± 0.26****	4.93 ± 0.20****	5.36 ± 0.35*,****

Notes: Results are mean ± SD, $n \geq 10$.
* $p < 0.05$ vs. normal control group.
** $p < 0.01$ vs. normal control group.
*** $p < 0.05$ vs. model control group.
**** $p < 0.01$ vs. model control group.

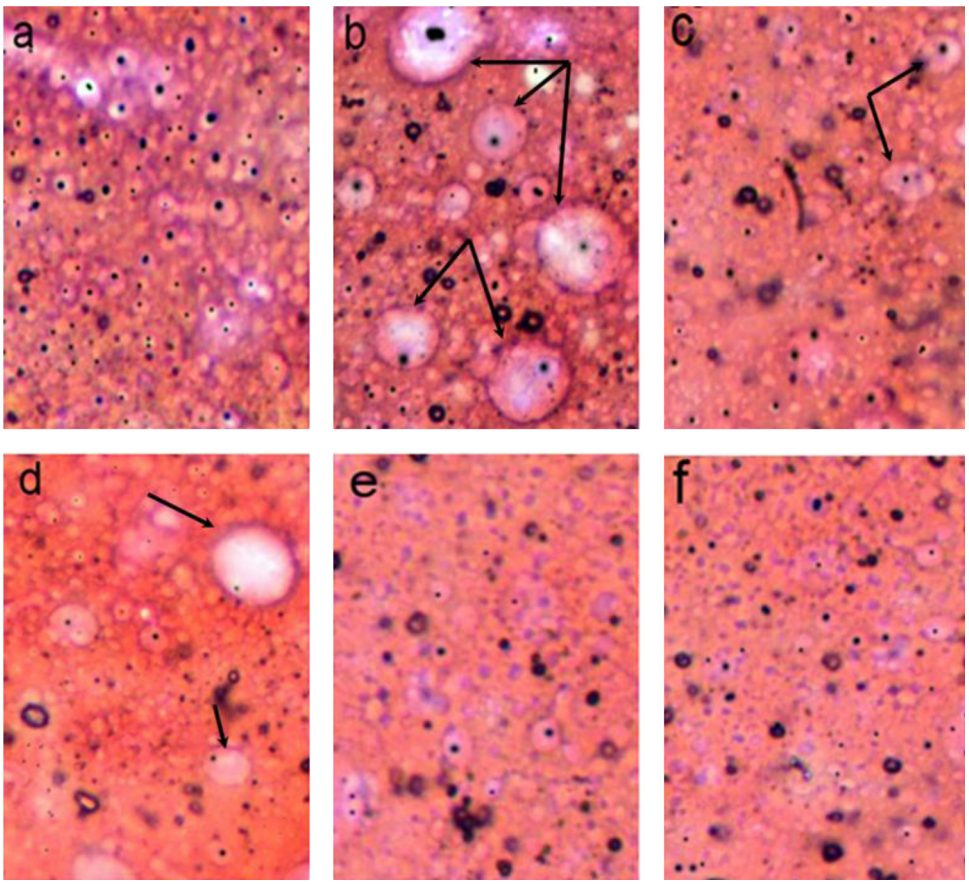

Fig. 7. Optical micrographs of mice liver tissues slice (magnification 40×). (a) Normal control group; (b) model control group; (c) positive control group; (d) LEP-1b group at 50 mg/kg; (e) LEP-1b group at 100 mg/kg; (f) LEP-1b group at 200 mg/kg. The black arrow indicates fat vacuoles.

control group, the high-dose, medium-dose as well as low-dose LEP-1b and the positive control drug of simvastatin all significantly increased the liver SOD activity and decreased the liver MDA content and liver index ($p < 0.01$ and $p < 0.05$). As shown in Table 3, the liver SOD activity of the high-dose LEP-1b group was significantly higher than that of the normal control group ($p < 0.05$), the liver MDA content and liver index of the high-dose LEP-1b mice was 22.44% lower and 4.26% higher than those of the positive control mice, respectively, and had no significant difference with those of the normal control group.

The differences in mice liver tissues slices from normal control group, model control group, positive control group and different LEP-1b groups were also compared by optical microscope after staining. As shown in Fig. 7, the liver cells of the normal mice are regularly arranged and have normal morphology, showing no symptoms of fat degeneration, whereas a great number of large fat vacuoles and invasive necrosis of cells are observed in the mice liver tissues of the model control group, showing obvious diffuse hepatic steatosis and inflammatory change. Liver tissue morphology of mice in the low-dose, medium-dose as well as high-dose LEP-1b groups and the positive control group were significantly recovered. The liver tissue morphology and arrangement of the high-dose LEP-1b mice showed no significantly difference from those of the normal mice, whereas there were still a small amount of fat vacuoles in mice of the low-dose LEP-1b group and the positive control group.

These results above indicated that LEP-1b effectively inhibited the increase of the serum ALT and AST activities, liver MDA content, and liver index of the model mice, and effectively improved the liver SOD activity. Additionally, optical micrographs of mice liver tissues slices suggested significant liver steatosis alleviating effects and liver tissue morphology restoring abilities of LEP-1b on liver tissue of the model mice, which fully demonstrates that LEP-1b can alleviate the peroxidation damage of liver tissues and promote the recovery of damaged liver tissues.

4. Conclusion

LEP-1b from *Lachnum* YM281 was isolated and purified. The molecular weight, structure and conformation of LEP-1b were studied and deduced. LEP-1b can also significantly decrease the serum lipids (TC, TG and LDL-C) and liver lipids (TC, TG and fat) levels of the model mice, reduce the serum ALT and AST activities and liver MDA content, and improve the liver SOD activity. These indicate that LEP-1b has a great blood–lipid reduction and hepatic lipid reduction effect and can promote the recovery of damaged liver tissues, and can be used in the development of lipid-reducing and liver-protecting drugs or health products. Further works on structure–activity relationship of LEP-1b are in progress.

Acknowledgments

This study was financially supported by the National Natural Science Foundation of China (No. 31070021) and the Fundamental Research Funds for the Central Universities (2012HGZY0020).

References

Bao, X. F., Wang, X. S., Dong, Q., Fang, J. N., & Li, X. Y. (2002). Structural features of immunologically active polysaccharides from *Ganoderma lucidum*. *Phytochemistry*, *59*, 175–181.

Cao, X. F., Yuan, T. Q., Sun, S. N., & Sun, R. C. (2011). Isolation and characterization of soluble polysaccharides from *Calamagrostis Angustifolia* Kom. *Bioresources*, *6*, 2896–2911.

Ding, H., Gao, Y., Chao, H., & Xia, D. (2010). Effect of polysaccharide from moso bamboo leaves on blood lipid of mice with hyperlipemia. *Food Science*, *31*, 259–262.

Dong, Q., Jia, L., & Fang, J. (2006). A β-D-glucan isolated from the fruiting bodies of *Hericium erinaceus* and its aqueous conformation. *Carbohydrate Research*, *341*, 791–795.

García-Mediavilla, V., Villares, C., Culebras, J. M., Bayón, J. E., & González-Gallego, J. (2003). Effects of dietary β-cyclodextrin in hypercholesterolaemic rats. *Pharmacology & Toxicology*, *92*, 94–99.

He, J. Z., Shao, P., Men, X. H., & Sun, P. L. (2010). Analysis of structural characteristics of polysaccharide from *Ganoderma lucidum*. *Chinese Journal of Analytical Chemistry*, *38*, 372–376.

He, Q., & Zhang, S. (2004). Advances in the studies on the mechanism of immunopotentiation effect of polysaccharides from edible-medicinal fungi. *Acta Edulis Fungi*, *11*, 52–58.

Hu, Y. B., Fu, X. J., Zhang, F. X., Ma, F. M., Wang, Z., & Xu, S. Y. (2010). Hypolipidemic study of xylanase-modified corn bran fibre in rats. *Food Chemistry*, *123*, 563–567.

Kritchevsky, D., & Tepper, S. A. (2005). Influence of a fiber mixture on serum and liver lipids and on fecal fat excretion in rats. *Nutrition Research*, *25*, 485–489.

Li, H., Zhang, M., & Ma, G. (2010). Hypolipidemic effect of the polysaccharide from *Pholiota nameko*. *Nutrition*, *26*, 556–562.

Li, J., Fan, L., & Ding, S. (2011). Isolation, purification and structure of a new water-soluble polysaccharide from *Zizyphus jujuba cv. Jinsixiaozao*. *Carbohydrate Polymers*, *83*, 477–482.

Luo, Y., Chen, G., Li, B., Ji, B., Guo, Y., & Tian, F. (2009). Evaluation of antioxidative and hypolipidemic properties of a novel functional diet formulation of *Auricularia auricula* and *Hawthorn*. *Innovative Food Science & Emerging Technologies*, *10*, 215–221.

Makishima, M., Okamoto, A. Y., Repa, J. J., Tu, H., Learned, R. M., Luk, A., et al. (1999). Identification of a nuclear receptor for bile acids. *Science*, *284*, 1362–1365.

Needs, P., & Selvendran, R. (1993). Avoiding oxidative degradation during sodium hydroxide/methyl iodide-mediated carbohydrate methylation in dimethyl sulfoxide. *Carbohydrate Research*, *245*, 1–10.

Percario, S., Odorizzi, V., Souza, D., Pinhel, M., Gennari, J., Gennari, M., et al. (2008). Edible mushroom *Agaricus sylvaticus* can prevent the onset of atheroma plaques in hypercholesterolemic rabbits. *Cellular and Molecular Biology*, *17*, 1055–1061.

Queiroz-Monici, K. S., Costa, G. E. A., Silva, N., Reis, S. M. P. M., & Oliveira, A. C. (2005). Bifidogenic effect of dietary fiber and resistant starch from leguminous on the intestinal microbiota of rats. *Nutrition*, *21*, 602–608.

Rout, D., Mondal, S., Chakraborty, I., & Islam, S. S. (2008). The structure and conformation of a water-insoluble (1 → 3)-,(1 → 6)-β-D-glucan from the fruiting bodies of *Pleurotus florida*. *Carbohydrate Research*, *343*, 982–987.

Shi, Z. J., Xiao, L. P., Deng, J., Xu, F., & Sun, R. C. (2011). Isolation and characterization of soluble polysaccharides of dendrocalamus brandisii: A high-yielding bamboo species. *Bioresources*, *6*, 5151–5166.

Suarez, E. R., Syvitski, R., Kralovec, J. A., Noseda, M. D., Barrow, C. J., Ewart, H. S., et al. (2006). Immunostimulatory polysaccharides from *Chlorella pyrenoidosa*. A new galactofuranan. Measurement of molecular weight and molecular weight dispersion by DOSY NMR. *Biomacromolecules*, *7*, 2368–2376.

Sun, Y., & Liu, J. (2009). Purification, structure and immunobiological activity of a water-soluble polysaccharide from the fruiting body of *Pleurotus ostreatus*. *Bioresource Technology*, *100*, 983–986.

Sun, Y., Liu, J., Yang, X., & Kennedy, J. (2010). Purification, structural analysis and hydroxyl radical-scavenging capacity of a polysaccharide from the fruiting bodies of *Russula virescens*. *Process Biochemistry*, *45*, 874–879.

Takahashi, N., Kawada, T., Goto, T., Yamamoto, T., Taimatsu, A., Matsui, N., et al. (2002). Dual action of isoprenols from herbal medicines on both PPARγ and PPARα in 3T3-L1 adipocytes and HepG2 hepatocytes. *FEBS Letters*, *514*, 315–322.

Tong, H., Xia, F., Feng, K., Sun, G., Gao, X., Sun, L., et al. (2009). Structural characterization and in vitro antitumor activity of a novel polysaccharide isolated from the fruiting bodies of *Pleurotus ostreatus*. *Bioresource Technology*, *100*, 1682–1686.

Thongngam, M., & McClements, D. J. (2005). Isothermal titration calorimetry study of the interactions between chitosan and a bile salt (sodium taurocholate). *Food Hydrocolloids*, *19*, 813–819.

Tseng, Y. H., Yang, J. H., & Mau, J. L. (2008). Antioxidant properties of polysaccharides from *Ganoderma tsugae*. *Food Chemistry*, *107*, 732–738.

Wang, C., Cui, J., & Wei, L. (2010). Effects of Artemisia capillary extract on hyperlipemia and liver fatty degeneration in Rats. *Chinese Archives of Traditional Chinese Medicine*, *28*, 1738–1740.

Wang, Y., Yin, H., Lv, X., Gao, H., & Wang, M. (2010). Protection of chronic renal failure by a polysaccharide from *Cordyceps sinensis*. *Fitoterapia*, *81*, 397–402.

Wilson, T. A., Nicolosi, R. J., Rogers, E. J., Sacchiero, R., & Goldberg, D. J. (1998). Studies of cholesterol and bile acid metabolism, and early atherogenesis in hamsters fed GT16-239, a novel bile acid sequestrant (BAS). *Atherosclerosis*, *140*, 315–324.

Ye, M., Li, S., Yang, L., Zhu, L., & Lin, Y. (2009). Study on extraction technology and antioxidative activity of polysaccharides produced by *Lachnum hyalopus*. *Journal of Zhejiang University (Agriculture and Life Sciences)*, *35*, 153–157.

Ye, M., Qiu, T., Peng, W., Chen, W., Ye, Y., & Lin, Y. (2011). Purification, characterization and hypoglycemic activity of extracellular polysaccharides from *Lachnum calyculiforme*. *Carbohydrate Polymers*, *86*, 285–290.

Yu, P., Li, N., Liu, X., Zhou, G., Zhang, Q., & Li, P. (2003). Antihyperlipidemic effects of different molecular weight sulfated polysaccharides from *Ulva pertusa* (Chlorophyta). *Pharmacological Research*, *48*, 543–549.

Zou, S., Zhang, X., Yao, W., Niu, Y., & Gao, X. (2010). Structure characterization and hypoglycemic activity of a polysaccharide isolated from the fruit of *Lycium barbarum* L. *Carbohydrate Polymers*, *80*, 1161–1167.